International Journal of Applied Engineering Research
ISSN 0973-4562 Volume 9, Number 24 (2014) pp. 30355-30364

http://www.ripublication.com

Formulation and Calculations for PbSe/PbSrSe Multiple Quantum Well Structures Total Losses

Majed Khodr

Department of Electronics and Communication Engineering, School of Engineering, American University of Ras Al Khaimah, P.O.Box 10021, Ras Al Khaimah, UAE, Fax +971 7 2210300,Tel: +971 2210500, majed.khodr@aurak.ae,

Abstract

In this work, we formulate, and calculate the total losses due to the free carrier absorption, optical waveguide scattering and the laser cavity end losses for PbSe/$Pb_{0.934}Sr_{0.066}$ Se quantum well laser structures. These losses were calculated for four structures of interest: SQW, MQW, MMQW and SCH-SQW. Our results will show that 1) the free carrier absorption losses are negligible, 2) the scattering losses are highest for MQW and MMQW structures, for a surface roughness amplitude of different values, and 3) the cavity losses are in an increasing order for the MQW (or MMQW) and SCH-SQW structures. These cavity losses are lowest for uncoated cavity ends. Coating these ends with a quarter wavelength BaF_2 layer increases the total cavity loss. In addition, coating the cavity ends with alternating quarter wavelength layers of BaF_2 and CaF_2 also results in an increase in the cavity loss. The increase in cavity loss due to coating is caused by the decrease in the mirrors' reflectivity values. These results show that coating with fluoride layers can best be utilized in applications where high transitivity values are needed.

1. Introduction

Breath analysis is a promising application and diagnostic tool that should perform well in clinical settings where real time breath analysis can be performed to assess patient health. Based on literature reports, health conditions such as Breast cancer and Lung Cancer have biomarker molecules in exhaled breath at wavelengths in the infra red (IR) region. A new technique that may play a key role in detecting these biomarkers is Tunable Laser Spectroscopy (TLS)[1-2]. Quantum nanostructure lasers, as part of TLS system, can be used to generate these critical wavelengths that can be absorbed by the various biomarkers molecules and hence detecting their presence in parts per million (ppm). Laser emission at these critical wavelengths is related to several system parameters.

A theoretical model was developed to conduct this study on PbSe/Pb $_{0.934}$ $Sr_{0.066}$ Se at (298 K) which is a promising nanostructure material system that have been used in clinical studies for detecting several biomarkers such as Asthma Biomarker (Nitric Oxide)[2]. Calculations of the energy levels, wavelength emission, gain, confinement factor, and current density assuming parabolic and non parabolic bands were previously published [3-4]. Moreover, the modal gain-current density relations were investigated for four quantum well structures: Single Quantum Well Lasers (SQW), Separate Confinement Heterostructure_Single Quantum Well Lasers (SCH_SQW), Multiple Quantum Well Lasers (MQW), and Modified Multiple Quantum Well Lasers (MMQW) [3-4]. However, the total losses that are needed for lasing to occur were not calculated.

In this work, these total losses due to free carrier losses, scattering losses, and end cavity losses for the four PbSe/Pb $_{0.934}$ $Sr_{0.066}$ Se quantum structures were calculated and analyzed. These results show that coating with fluoride layers can best be utilized in applications where high transitivity values are needed as shown in the two proposed design structures.

2. Total Losses Calculations

In laser oscillators, the concern is with the modal gain rather with the maximum gain. The modal gain is defined as the gain experienced by the traveling laser mode. It is obtained by multiplying the maximum gain values by the confinement factor. The optical confinement factor depicts the overlap of the optically guided wave with the quantum well. In order for laser oscillation to occur, the modal gain $g_{\mathrm{mod}}(\hbar\omega)$ at the lasing photon energy $\hbar\omega$ must equal the total losses α_{total} according to the following equation:

$$g_{\mathrm{mod}}(\hbar\omega) = \alpha_{total}\,. \tag{1}$$

Therefore, the oscillation condition requires sufficient gain to overcome the total losses. The total loss is given by [5]:

$$\alpha_{total} = \Gamma_o^{QW}\alpha_{fc} + \alpha_s + \frac{1}{2L}\ln\frac{1}{R_1R_2} \tag{2}$$

and the gain oscillation condition is written as:

$$g_{\mathrm{mod}}(\hbar\omega) = \Gamma_o^{QW}\alpha_{fc} + \alpha_s + \frac{1}{2L}\ln\frac{1}{R_1R_2}\,. \tag{3}$$

where Γ_o^{QW} is the confinement factor for the particular structure, α_{fc} is the free carrier absorption and α_s is the scattering loss due to waveguide imperfections. The loss due to radiation from the ends of the laser is given by:

$$\alpha_c = \frac{1}{2L} \ln \frac{1}{R_1 R_2}$$

where L is the laser cavity length and R_1 and R_2 are the end facet reflectivities.

2.1 Free carrier absorption

Free carrier absorption is crucial to semiconductor lasers because it is a major unavoidable loss mechanism. It results from the scattering of carriers in motion and is therefore influenced by the same scattering mechanisms that influence carrier mobility [5]. An expression for free carrier absorption in lead salts has been given by Anderson [6]:

$$\alpha_{fc} = \frac{N_n e^3}{n_r c \varepsilon_o \mu_n (m_w^*)^2 (\hbar\omega)^2} . \tag{4}$$

N_n is the carrier concentration, μ_n is the carrier mobility, $\hbar\omega$ is the emitted photon energy, n_r the index of refraction and m_w^* is the conductivity effective mass in the active region. The constants *e, c* and ε_o are, electron charge, speed of light and permittivity of free space, respectively. Substituting for these constants in Eq.(4) with the proper units gives :

$$\alpha_{fc} = 8 \times 10^{-17} \frac{N_n}{n_r \mu_n (m_w^*)^2 (\hbar\omega)^2} (1/cm) . \tag{5}$$

Typical values of the carrier concentrations and mobilities in lead salts films are $\cong 10^{17} cm^{-3}$ and $\cong 10^4 cm^2 \cdot V^{-1} \cdot \sec^{-1}$ [7]. Substituting these values and n_r=4.9, m_w^*=0.0.08, and $\hbar\omega$=0.3 eV into Eq. (5), we calculate the free carrier absorption value $\alpha_{fc} \cong 0.3(1/cm)$. This is a small loss value when multiplied by the confinement factor for a QW structure (typical value of $\cong 0.03$), thus the first term in Eq.(3) can be neglected. Therefore, the losses due to free carrier absorption in QW structures are negligible, mainly because of the small confinement factor [4].

2.2 Scattering losses

The scattering loss α_s is due to scattering of radiation out of the optical waveguide by either non planar heterostructure interfaces or imperfections in the dielectric layers [5]. Several mathematical models of discrete and continuous waveguide deformations from which optical scattering losses were computed as functions of parameters which characterize the severity of the imperfection can be found in reference [8]. Here, however, only the terrace discontinuities in the thickness of the active layer waveguide will be discussed. The growth of terraces on the wafer top surface depends upon slight random misorientations of the substrate [8]. For a given wafer the periodicity of such terrace structures on the surface can vary from 10 to 50 μm

with peak-to-valley heights (roughness amplitude) of $\cong$ 50 nm, as shown in the inset of Fig. 1. In this figure, a step-function discontinuity in the thickness of the active region reminiscent of one terrace.

The optical scattering loss due to this terrace is given by [8]:

$$\alpha_S = \frac{r}{L}\ln(\frac{1}{1-\Delta P/P}), \tag{6}$$

where r is the number of uncorrelated identical defects in a cavity of length L ($r \cong 10$ periods along the length of any given laser [8]). The quantity $\Delta P/P$ is the fraction of the optical power, incident upon a discrete waveguide imperfection, which is scattered (radiated out of the guide). In terms of the effective waveguide thickness d_e, which is nominally measured from the peak of the electric field to the place where the field has fallen to 1/e of its peak value, $\Delta P/P$ is given by [8]:

$$\frac{\Delta P}{P} = 1 - 4(\frac{d_{e1}}{d_{e2}} + \frac{d_{e2}}{d_{e1}})^{-2} \tag{7}$$

where

$$d_{ei} = d_i(1 + 1/\gamma d_i). \tag{8}$$

Defining:

$$V \equiv \sqrt{n_{r,1}^2 - n_{r,2}^2}(\frac{2\pi}{\lambda})d_i \tag{9}$$

then

$$\gamma d_i = \frac{1}{2}[\sqrt{(4V^2 + 1)} - 1] \tag{10}$$

for the lowest order TE mode in the waveguide. The active layer thickness $\bar{t} = 2d_2$ and its index of refraction $\bar{n} = n_{r,1}$. The cladding layers have an index of refraction $n_c = n_{r,2}$. The roughness amplitude is denoted by A and it is has the same value around the active region (Fig. 1).

Using the above formulas an estimated value of the optical scattering loss can be calculated for PbSe/Pb $_{0.934}$ Sr$_{0.066}$ Se MQW and PbSe/Pb $_{0.934}$ Sr$_{0.066}$ Se/ BaF_2 SCH structures [4]. As shown in Fig 1, the calculated scattering losses for PbSe/Pb $_{0.934}$ Sr$_{0.066}$ Se MQW structure decreases with increasing number of wells and decreasing the roughness amplitude. For number of wells N_w=5 and above these scattering losses are very small and can be ignored.

For a fixed cavity length L=250 μ m, well width *w*=10 nm, barrier thickness B=2.5 nm, number of wells N_w=5, emission wavelength of 3.9 μ m, a value of $Lc \cong 0.2\mu m$ (for SCH structure only), and roughness amplitudes A of 10 nm and 50 nm, the calculated α_s for the three structures are shown in Table (I). The MQW and MMQW structures do not differ much, however both values differ substantially from α_s for the SCH structure. Thus, although a high confinement factor is obtained for the MQW structures over the SCH [4], the scattering losses are higher.

In addition, careful experimental procedures are needed to achieve defect free interface layers in order to reduce optical scattering from the waveguide. Growing a laser structure on a rough substrate surface can affect the performance of the device. The growth of terraces is one of the defects that can exist at the interface. Other defects, such as growth voids, can exist at the interface layers and the theoretical formulation for calculating α_s due to these defects is found in Ref.[8]

2.3 Cavity end losses

The last term in the expression for the total loss α_{lotal} Eq.(3) represents the loss from the end facets of the laser cavity. The power reflectivity of the end mirrors R_1 and R_2 can be calculated by using Fresnel relations [9] or an uncoated end, the power reflectivity is given by:

$$R = \left(\frac{\overline{n_r} - n_a}{\overline{n_r} + n_a}\right)^2 \tag{11}$$

where $\overline{n_r}$ is the index of refraction of the laser active region and n_a is the index of refraction of air (1.0). For a coated end, the standard expression for calculating the reflectivity of a quarter wavelength thin film is [10]

$$R = \left(\frac{n_f^2 - n_a \overline{n}_r}{n_f^2 + n_a \overline{n}_r}\right)^2 \tag{12}$$

where n_f is the index of refraction of the film.

For the PbSe/Pb $_{0.934}$ Sr$_{0.066}$ Se MQW structures with a well width *w*=10 nm, a barrier thickness B=2.5 nm and a number of wells N_w=5, the reflectivity of the uncoated ends is $R \cong 0.4$. The reflectivity from the uncoated ends of the PbSe/Pb $_{0.934}$ Sr$_{0.066}$ Se / BaF_2 SCH structure with *w*=10 nm and $Lc \cong 0.2\mu m$ is $R \cong 0.2$ (Table 2). The difference between the two structures is due to the difference of the average index of refraction calculated ($\overline{n_r}$ =4.5) for MQW structure and ($\overline{n_r}$ =2.6) for SCH structure [4]. Thus, for an uncoated end, the last term in the total loss expression Eq.(3) is higher for the SCH structure over its counterpart, the MQW structures, at a fixed cavity length *L*. The values of α_c for the MQW and SCH structures with *L*=250 μ m

are $\cong$ 36 cm^{-1} and $\cong 64$ cm^{-1} (Table 3).

Coating the laser cavity ends with a quarter wavelength BaF_2 ($n_f \cong 1.46$ near the infrared region) single thin film, the calculated mirror reflectivity from Eq.(12) for the MQW structure is $R \cong 0.13$ and that for the SCH structure is $R \cong 0.01$ (Table 2). Therefore, coating the end facets with a BaF_2 thin film increases the total losses in the waveguide region. The values of α_c for the MQW and SCH structures with L=250 μm are $\cong$ 82 cm^{-1} and $\cong 184$ cm^{-1} (Table 3). Assuming these fluoride films have zero absorption in the near infrared region, the transmittance T=1-R is high and thus they can be useful for optically pumping the above QW structures. Coatings of multilayer quarter wavelength thin films with an alternating high index of refraction n_H and low index of refraction n_L can be used to increase the tramsmissivity or the reflectivity of the film. This type of coating is referred to as anti reflection (AR) coating and the reflectivity can be calculated using the following formula [9]:

$$R = \left(\frac{n_a (n_H / n_L)^N - \overline{n_r}}{n_a (n_H / n_L)^N + \overline{n_r}}\right)^2 \tag{13}$$

where N is the number of layers. Alternating layers of BaF_2 ($n_H \cong 1.46$) and CaF_2 ($n_L \cong 1.40$) in the near infrared region) can be grown on the end facets of the above structures.

For N=2, the reflectivity values of the MQW structure is $R \cong 0.37$ and that for the SCH structure is $R \cong 0.17$ (Table 2. These values are close to the values found using Eq.(11) for the uncoated case. For N >2, the reflectivity decreases. For N=4, $R \cong 0.34$ ($T \cong 0.57$) for the MQW structure and $R \cong 0.14$($T \cong$ 0.86) for the SCH structure (Table 3). The reflectivity decreases for N >2 because $n_a (n_H / n_L)^N < \overline{n_r}$ for all N. However, assuming zero absorption, anti reflecting coatings of fluoride layers can best be utilized in applications where high transmitivity values are needed. In order to use anti reflection coatings in applications where high reflectivity values are needed, $n_a (n_H / n_L)^N > \overline{n_r}$ for all N. The values of α_c for the MQW and SCH structures for AR coating are listed in Table 3. From the last term of Eq. (3), in order to reduce the mirror losses, one must increase the mirrors' reflectivity values and increase the cavity length.

Using Tables 1 and 3, figure 2 shows the total losses ignoring the free carrier absorption losses and considering amplitude roughness of 50 nm. The maximum losses were noticed for the coated structures and these losses decrease with increasing the number of wells. For number of wells N_w=5 and above cavity losses values exceeds the scattering losses and eventually dominate and a fixed minimum total losses are reached for the system independent of the number of wells. For the SQW-SCH structure, one can obtain the total losses by adding those corresponding values from tables 1 and 3. These value are 66.76 (1/cm), 186.76 (1/cm, 73.76 (1/cm), and 81.76 (1/cm) for uncoated, coated, AR coating (N=2), and AR coating (N=4), respectively.

A principal feature of the QW laser is the extremely high optical gain that can be obtained for very low current densities. Equally important, however, in determining laser properties are modal gain, determined by the optical confinement factor, and the ability to collect injected carriers efficiently [4]. These latter factors prevent the improvement of laser performance for arbitrarily thin QW dimensions unless additional design features are added. These design improvements include the use of multiple QW's (MQW) and /or the separate confinement heterostructure (SCH) scheme where optical confinement is provided by a set of optical confinement layers, while carrier confinement occurs in another embedded layer. The structures under study are shown in Fig.1a where the well material is PbSe, the barrier material is $PbSe_{0.934}Te_{0.066}$ and the cladding material can be the barrier material itself or any lattice matched material to the structure. The refractive index profile depicted in Fig. 1b is illustrative of the devices under consideration. For the MQW structure, the index of refraction of the barrier material is the same as the cladding material ($n_{r,c} = n_{r,B}$). For the MMQW structure $n_{r,c} < n_{r,B}$.

The last structure, in which a single-quantum well active layer is embedded in a step-index wave-guide layer, which in turn is sandwiched between outer cladding layers, is called a step index-SCH structure. The step index graded layer thickness is denoted by Lc in Fig. 1a. The barrier material system $Pb_{0.934}Sr_{0.006}Se$ parameters used in this study are: the energy gap 0.46 eV, index of refraction 2.43 and effective mass 0.142, while the well material system PbSe parameters used in this study are: the energy gap 0.28 eV, index of refraction 4.93 and effective mass 0.082, and the cladding material used for the MMQW and SQW_SCH structures is BaF_2 with an index of refraction of 1.46 [3, 5, 6].

3. Design Proposal

As shown in sec 2.3, the fluoride layers are useful as anti-reflection coatings. Also, they are lattice matched with silicon and therefore can be used as buffer layers between the structure and silicon substrates. The IV-VI semiconductor structure studied here PbSe/ $PbSe_{0.934}Te_{0.066}$ can be electrically or optically pumped as proposed in figure 3 (a) and (b). It was shown in section 2.3 above that optical pumping can be done from the side where alternating high index/low index fluoride antireflection coating is grown. Also, optical pumping can be done from the top of the structure and the structure can be grown sandwiched between pairs of alternating high and low refractive index layers of $PbSe_{0.934}Te_{0.066}/BaF_2$ distributed Bragg reflector (DBR) on the bottom and pairs of $PbSe_{0.934}Te_{0.066}/BaF_2$ DBR on top, all epitaxially grown on CaF_2/Si (111) Substrate. The BaF_2 capping layer on top of the structure can be grown to prevent oxidation of strontium. These fluoride layers are useful as anti-reflection coatings in optically pumping these structures as noted from this study.

4. Summary and Conclusion

The total losses due to the free carrier absorption, optical waveguide scattering and

the laser cavity were calculated for MQW, MMQW, and SQW_SCH quantum well structures. The small confinement factor value causes the free carrier absorption loss to be negligible, however the scattering and cavity losses can't be neglected and need to be considered in the threshold current calculations, which will be kept for future publication. Finally, it was shown that fluoride films have zero absorption in the near infrared region, and thus they can be useful for optically pumping the above QW structures.

Table 1: The scattering loss due to a step terrace for the MQW, MMQW and SCH-SQW structures.

Amp. rough. (nm)	α_s, MQW (1/cm)	α_s, MMQW(1/cm)	α_s, SCH (1/cm)
10	2.4	2.3	0.09
50	25	16	2.76

Table 2: Mirror reflectivity values for the MQW, MMQW and SCH-SQW structures. The reflectivity R is for both ends of the laser cavity.

	R, MQW	R, MMQW	R, SCH
Uncoated	0.4	0.4	0.2
Coated	0.13	0.13	0.01
AR coating (N=2)	0.37	0.37	0.17
AR coating (N=4)	0.34	0.34	0.14

Table 3: Cavity losses for the MQW, MMQW and SCH-SQW structures. The laser cavity length is 250 μm for all the structures.

	α_c, MQW (1/cm)	α_c, MMQW(1/cm)	α_c, SCH (1/cm)
Uncoated	36	36	64
Coated	82	82	184
AR coating (N=2)	40	40	71
AR coating (N=4)	43	43	79

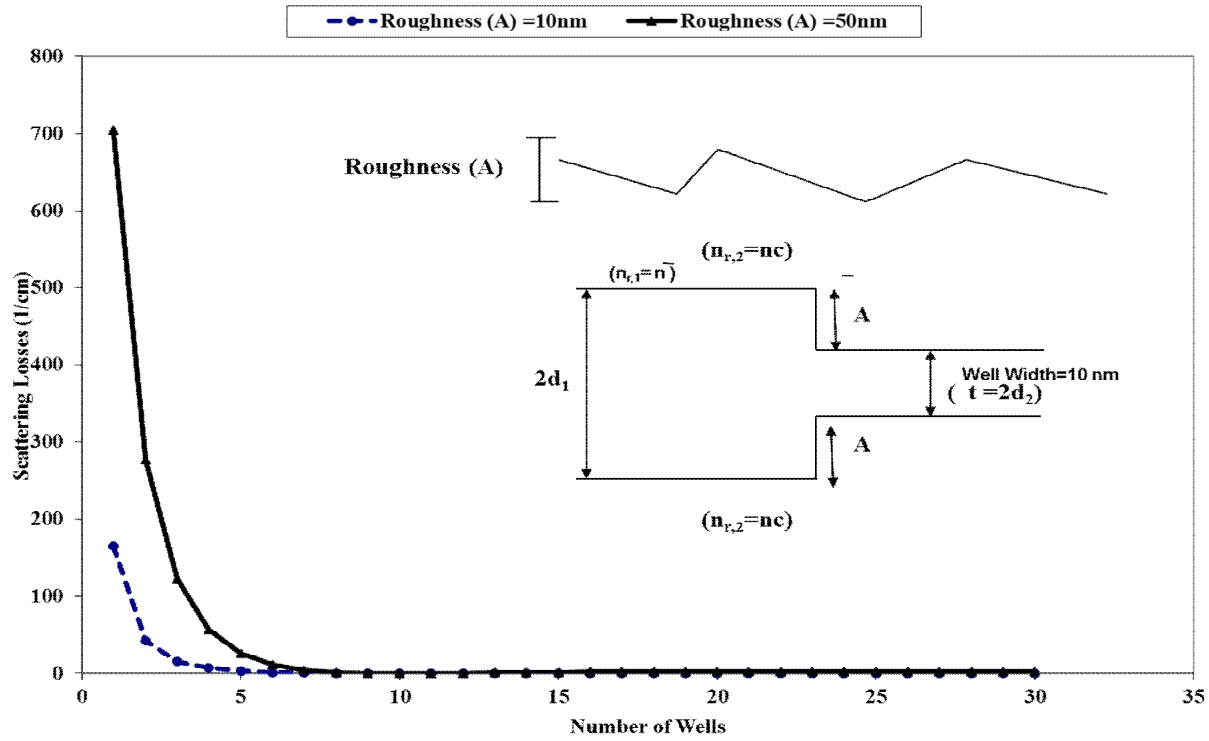

Fig 1. The scattering losses decrease with an increase in number of wells for roughness amplitudes 10 nm and 50 nm. The inset shows the step terrace model and roughness amplitude. Well width is 10 nm.

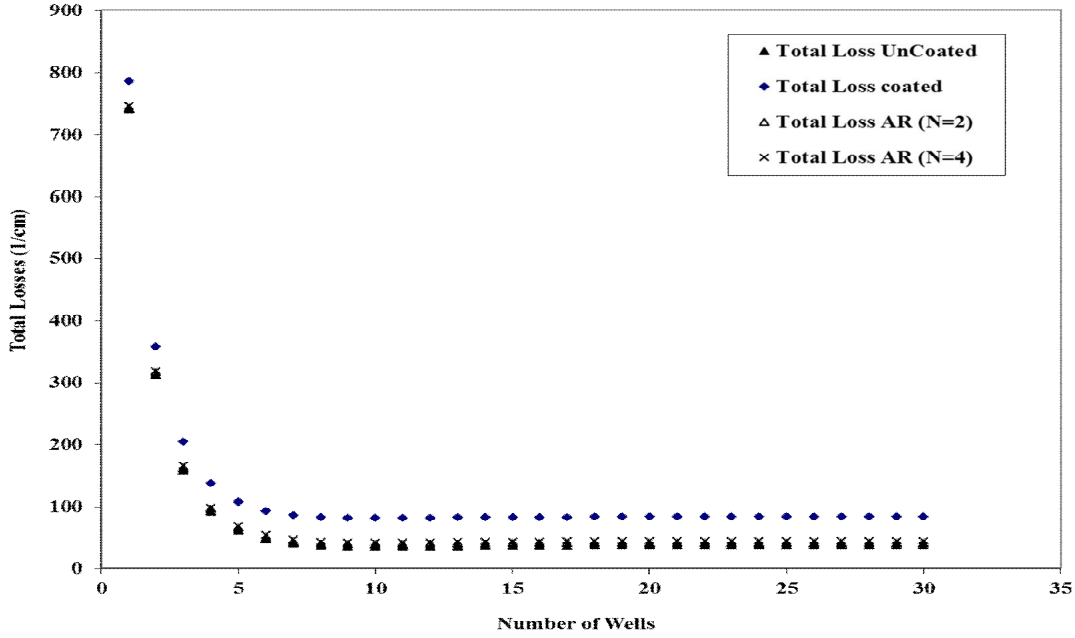

Fig. 2: The total losses as a function of number of wells shows the minimum loss values at which cavity losses dominate all other losses in the system. Well width is 10 nm and roughness amplitude is 50 nm.

List of References

1. C. B. Roller, K. Namjou, J. Jeffers, M. Camp, P. J. McCann, and J. Grego, “Nitric oxide breath testing using tunable diode laser absorption spectroscopy: Application in respiratory inflammation monitoring” Applied Optics,vol. 41, 6018 (2002).
2. P. J. McCann, K.Namjou, C.Roller, G. McMillen, and P. Kamat, “ IV-VI Semiconductor Lasers for Gas Phase Biomarker Detection” Proceedings of SPIE, 6756, 675603-1 (2007).
3. M. F. Khodr, P. J. McCann, "Theoretical Analysis and Design of PbSe/PbSrSe Quantum Well Structures for Fabricating Tunable Mid-Infrared Lasers,” International Journal of Applied Engineering Research, Vol. 9, Number 17, 4065 (2014).
4. M. F. Khodr, " Confinement Factor Calculations for SQW, SCH_SQW, MQW, and MMQW PbSe/PbSrSe Quantum Well Structures,” International Journal of Applied Engineering Research, Vol. 9, Number 21, 11413 (2014).
5. H. C. Casey and M. B. Panish, Heterostructure Lasers Part A: Fundamental Principles, Acadimic Press, New york (1978).
6. W. W. Anderson, "Gain-ferquency-current relation for double heterostructure lasers," IEEE J. Quantum Electron., 13, 532 (1977).
7. W. Shen, et al., “ Band gaps, effective masses and refractive indices of PbSrSe thin films: Key properties for mid-infrared optoelectronic devices applications”, J. of Appl. Phys., vol. 91, pp192-198, (2002)
8. F. R. Nash, W. R. Wagner and R. L. Brown, "Threshold current variations and optical scattering losses in (Al,Ga)As double-heterostructure lasers," J. Appl. Phys., 47, 3992 (1976).
9. O. S. Heavens, Optical Properties of Thin Solid Films, Dover Publications Inc., New York (1991).
10. I. M. Thomas, "Method for the preparation of porous silica antireflection coatings varying in refractive index from 1.22 to 1.44," appl. Opt., 31, 6145 (1992).